# One-dimensional antiferromagnetism in fluoro-gallium phthalocyanine-$(BF_4)_{0.25}$

Ichiro Hiromitsu, Nobuhisa Ikeda, Makoto Handa, and Takashi Ito
*Department of Material Science, Interdisciplinary Faculty of Science and Engineering, Shimane University, Matsue 690, Japan*
(Received 2 September 1997; revised manuscript received 25 November 1997)

The crystal structure and magnetism of fluoro-gallium phthalocyanine (GaPcF) doped with $BF_4$ are studied. A powder x-ray-diffraction analysis indicates that the stoichiometry is GaPcF-$(BF_4)_{0.25}$ and that the unit cell is a tetragonal of $a=18.832\pm0.019$ Å and $c=7.592\pm0.012$ Å in which the GaPcF polymer axes run parallel to the $c$ axis. The phthalocyanine rings have an interleaved structure, i.e., the rings in the nearest-neighbor chains have different $c$ coordinates. The $BF_4^-$ ions occupy their sites randomly with a probability of 0.25. The electron paramagnetic resonance (EPR) signal intensity and the linewidth do not show any anomaly between 4.2 and 300 K, indicating that no magnetic transition occurs. The EPR signal intensity at 300 K indicates that the spins are localized. The temperature dependence of the static magnetic susceptibility is explained by the random-exchange Heisenberg antiferromagnetic chain (REHAC) model. An analysis on the REHAC model shows that the GaPcF-$(BF_4)_{0.25}$ is a one-dimensional antiferromagnet in which the exchange interaction is randomly disordered in such a way that, on the average, 25% of the nearest neighbor spins have an interaction of 40% strength compared to the others. The one dimensionality is attributed to the interleaved structure and to the random distribution of the $BF_4^-$ ions with a possible partial correlation. [S0163-1829(98)04614-1]

## I. INTRODUCTION

Acceptor-doped phthalocyanines have been extensively studied because of their high electric conductivity and also their interesting magnetism. A typical example of the highly conductive phthalocyanine is nickel-phthalocyanine iodide (NiPc-I).[1,2] The NiPc-I shows a conductivity of $\sim 500\ \Omega^{-1}\mathrm{cm}^{-1}$ at room temperature and retains a metallic band structure down to a temperature below 2 K showing Pauli paramagnetism.[2] In the NiPc-I, the phthalocyanine (Pc) rings form a cofacially stacked one-dimensional array,[1] on which the charge transport occurs with a strongly one-dimensional character.

Fluoro-aluminum-phthalocyanine iodide (AlPcF-I),[3–5] on the other hand, shows totally different transport and magnetic properties from those of NiPc-I although AlPcF-I has an isomorphous crystal structure with NiPc-I: AlPcF-I shows a nonmetallic charge transport and exhibits three-dimensional (3D) antiferromagnetism with a Néel temperature ($T_N$) of 80 K. The difference between AlPcF-I and NiPc-I is attributed to the difference in the inter-ring distance along the Pc chain, i.e., 3.55 and 3.24 Å for AlPcF-I and NiPc-I, respectively. The longer inter-ring distance for AlPcF-I causes a narrower bandwidth, which makes the electron correlation effect more important. Thus, AlPcF-I is considered to be a Mott insulator.[6] The localization of the spins makes the interspin exchange interaction effective, resulting in 3D antiferromagnetism in the case of AlPcF-I. Then, the question of whether the three dimensionality in the magnetism is a common feature of the acceptor-doped phthalocyanines as long as the spins are localized arises, which is the point of the present paper.

In the present study, the crystal structure and magnetism of $BF_4$-doped fluoro-gallium phthalocyanine [GaPcF-$(BF_4)_{0.25}$] are studied. The GaPcF is a cofacially stacked polymer phthalocyanine with a $[\text{-Ga-F-}]_n$ backbone,[7,8] being isomorphous with AlPcF. It will be shown that the spins in GaPcF-$(BF_4)_{0.25}$ are localized as in the case of AlPcF-I but the magnetism is one dimensional (1D). The difference in the dimensionality is attributed to differences in the crystal structure. Thus, it will be demonstrated that the dimensionality is affected by structural factors.

The crystal structure and charge transport properties of GaPcF-$(BF_4)_x$ have already been reported by Futamata *et al.*[9] They interpret the magnetic susceptibility of GaPcF-$(BF_4)_x$ as a sum of the Pauli and Curie components, which is often the case for many conductive polymers. They assume that the Pauli component is independent of temperature and estimate from what they assume to be the Pauli susceptibility that the bandwidth is 0.14 eV. However, their interpretation is not self-consistent since the Pauli susceptibility is temperature dependent with a bandwidth as narrow as 0.14 eV.[10] It is also quite doubtful that metallic charge transport occurs with a bandwidth of only 0.14 eV. Since they do not show the explicit experimental data of the temperature dependence of the susceptibility, only limited information is obtained from their paper about the magnetism. Furthermore, the crystal structure proposed by Futamata *et al.* does not give a satisfactory fit to the experimental x-ray diffraction data. The present study gives an improved analysis of the crystal structure and shows that the spins are localized.

## II. EXPERIMENT

GaPcF was synthesized using a procedure from the literature[11] and was purified by subliming three times at 490 °C in a vacuum of $10^{-2}$ Pa. After this purification, GaPcF did not have any impurity spins detectable by electron paramagnetic resonance (EPR). $NOBF_4$ was purchased from Aldrich Chemical Co. and was used without further purification.

The GaPcF-$(BF_4)_x$ powder was synthesized by reacting GaPcF with $NOBF_4$ (Refs. 9 and 12): GaPcF and $NOBF_4$ with a molar ratio of 1:1 was mixed in a flask, into which

 

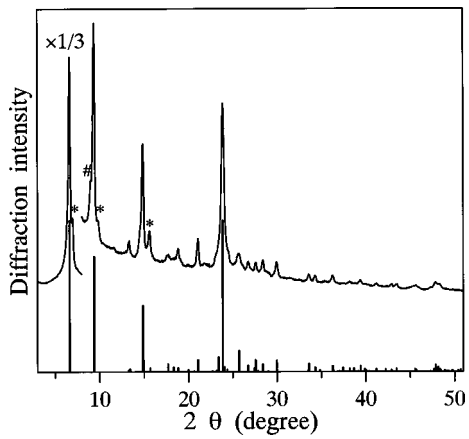


FIG. 1. Powder x-ray diffraction pattern of GaPcF-$(BF_4)_{0.25}$ with Cu-$K\alpha$ radiation. * denotes the reflection of the nondoped-GaPcF phase. ♯ denotes a reflection of unknown origin. The bars show the theoretical diffraction intensities for the crystal structure in Fig. 2.

degassed dichloromethane was introduced by vacuum distillation. The mixture was stirred at 20 °C for 22 h in Ar gas, then filtered. Finally, the product on the filter paper was dried by pumping with a rotary pump. The sample was not washed with any solvent since the $BF_4^-$ ions are easily removed from the sample.[9] The stoichiometry of the obtained product is GaPcF-$(BF_4)_{0.25}$ determined by an x-ray diffraction analysis as described in Sec. III A.

The powder x-ray diffraction measurement was done on a Rigaku RINT2100 diffractometer using Ni-filtered Cu-$K\alpha$ radiation. The $K\alpha_2$ contribution to the diffraction intensity was subtracted analytically from the neat diffraction intensity using the Rachinger method.[13] The receiving slit was set at 0.15 mm, and the divergence and the scattering slits were set at 0.5° for $2\theta=3°-30°$, 1° for $2\theta=23°-50°$, and 2° for $2\theta=40°-65°$. The analysis of the crystal structure was done using the program XRAY for a personal computer originally made in our laboratory, the details of which are described elsewhere.[3,14] In the analysis, a temperature factor of $\exp[-8(\sin\theta/\lambda)^2]$ was assumed for the diffraction intensity, referring to a temperature factor of NiPc-I.[1]

The EPR measurement was done on a homemade *K*-band (24 GHz) apparatus with a $TE_{111}$ cylindrical cavity employing a 100-kHz field modulation of 0.2 G. The sample was sealed at 760 Torr with high-purity He gas. The temperature dependence of the EPR signal intensity was determined by measuring the relative intensity of the sample to that of $K_3CrO_8$, which obeys the Curie-Weiss law with a Weiss temperature of $-2.7$ K.[15] The $g$ value and the effective spin number were determined using diphenylpicrylhydrazyl[16] (DPPH) as a standard sample.

The static susceptibility measurement was done with the Faraday method using a Cahn 2000 Electro-Balance system. The vacuum chamber containing the sample was filled with high-purity He gas of 710 Torr before cooling down the sample to liquid-He temperature. The sensitivity of the Cahn 2000 system was calibrated using the standard sample $[Ni(H_2NCH_2CH_2NH_2)_3]S_2O_3$.[17] The diamagnetic correction of GaPcF-$(BF_4)_{0.25}$ was done using a measured susceptibility of pristine GaPcF and an estimated one of $BF_4$ from the Pascal constants. All the measurements at variable temperature were made by increasing the temperature from 4.2 K.

TABLE I. X-ray-diffraction data for the GaPcF-$(BF_4)_{0.25}$.

| $(hkl)$ | $2\theta_{obs}$ | $2\theta_{calc}$ | $I_{obs}$ | $I_{calc}$ |
|---|---|---|---|---|
| (110) | 6.65 | 6.63 | 1 | 1 |
| (200) | 9.40 | 9.38 | 0.2575 | 0.2541 |
| (220) | 13.32 | 13.28 | 0.0134 | 0.0033 |
| (111) | [a] | 13.41 | [a] | 0.0056 |
| (310) | 14.87 | 14.86 | 0.1478 | 0.1457 |
| (201) | [a] | 14.97 | [a] | 0.0242 |
| (221) | 17.70 | 17.70 | 0.0089 | 0.0172 |
| (400) | 18.83 | 18.83 | 0.0191 | 0.0087 |
| (311) | [a] | 18.92 | [a] | 0.0017 |
| (420) | 21.07 | 21.07 | 0.0321 | 0.0262 |
| (102) | 23.87 | 23.88 | 0.2356 | 0.3329 |
| (212) | 25.69 | 25.71 | 0.0221 | 0.0470 |
| (440) | 26.75 | 26.75 | 0.0087 | 0.0139 |
| (530) | 27.58 | 27.59 | 0.0093 | 0.0258 |
| (600) | 28.39 | 28.40 | 0.0107 | 0.0169 |
| (620) | 29.97 | 29.97 | 0.0194 | 0.0252 |
| (710) | 33.61 | 33.61 | 0.0078 | 0.0174 |
| (640) | 34.28 | 34.30 | 0.0063 | 0.0090 |
| (730) | 36.27 | 36.29 | 0.0095 | 0.0124 |
| (800) | 38.20 | 38.19 | 0.0032 | 0.0050 |
| (731) | [a] | 38.23 | [a] | 0.0018 |
| (820) | 39.39 | 39.41 | 0.0050 | 0.0126 |
| (750) | 41.20 | 41.19 | 0.0033 | 0.0059 |
| (840) | 42.91 | 42.90 | 0.0014 | 0.0039 |
| (910) | 43.44 | 43.46 | 0.0038 | 0.0069 |
| (812) | 45.52 | 45.54 | 0.0056 | 0.0035 |
| (742) | [a] | 45.54 | [a] | 0.0025 |

[a]The reflection overlaps with the neighboring reflection. For example, the (111) and the (220) reflections are not resolved, so that the listed value of the $I_{obs}$ for (220) is the sum of the intensities of the two reflections.

## III. RESULTS

### A. Powder x-ray diffraction

Figure 1 shows the x-ray-diffraction pattern of the GaPcF-$(BF_4)_x$ powder. In Fig. 1, the weak peaks at $2\theta=6.98°$, 9.86° and 15.65° are those of pristine GaPcF, indicating that the sample contains only a small amount of the nondoped phase. The weak reflection at $2\theta=8.96°$ is a reflection of unknown origin whose intensity slightly depends on the samples. All the other reflections in Fig. 1 are indexed with a tetragonal unit cell of $a=18.832\pm0.019$ Å and $c=7.592\pm0.012$ Å as shown in Tables I and II. In Table I, good agreement is seen between the observed and the calculated diffraction angles.

In order to find the structural arrangement of the Pc rings and $BF_4^-$ in the unit cell, the theoretical diffraction intensities on a series of structural models have been compared with the experimental ones. The best fit is obtained with the structure shown in Fig. 2. In this structure, the unit cell contains four Pc rings, and the GaPcF-polymer chains run parallel to

TABLE II. Crystallographic data of the GaPcF-$(BF_4)_{0.25}$.

| Stoichiometry | Crystal system | $Z$ | Unit-cell parameters | Staggering angle |
|---|---|---|---|---|
| GaPcF-$(BF_4)_{0.25}$ | tetragonal | 4 | $a=18.832\pm0.019$ Å<br>$c=7.592\pm0.012$ Å | 15° |

[a]The number of the Pc rings in the unit cell.

the $c$ axis. The two Pc rings adjacent along the $c$ direction have an inter-ring spacing of 3.80 Å and are staggered[18] by 15°, which is the angle between the trans N-Ga-N vectors of the two Pc rings. The Pc-ring arrays of the nearest-neighbor Pc chains have an interleaved structure,[18] i.e., the Pc rings on the neighboring chains have different $c$ coordinates: The four Pc rings in the unit cell are located at (0, 0, 0), (0, 0, 0.5$c$), (0.5$a$, 0.5$a$, 0.2$c$), and (0.5$a$, 0.5$a$, 0.7$c$). $BF_4^-$ ions, on the other hand, occupy their sites randomly with a probability of 0.25 so that the stoichiometry becomes GaPcF-$(BF_4)_{0.25}$. The determination of the stoichiometry of $x=0.25$ was possible since the intensities of the (200) and the (310) peaks are quite sensitive to the value of $x$. The explicit $c$ coordinates of the $BF_4^-$ sites, however, are unknown since powder x-ray diffraction is insensitive to the $c$ coordinates of them. The theoretical diffraction pattern for this structure is shown in Fig. 1, and the experimental and the theoretical diffraction intensities are listed in Table I. Reasonable agreement is seen between theory and experiment.

The stoichiometry of $x=0.25$ does not depend on the samples: When GaPcF is reacted with a smaller amount of $NOBF_4$ than the molar ratio of 1:1, the fraction of the nondoped phase increases, but the stoichiometry of the doped phase is always GaPcF-$(BF_4)_{0.25}$. This may indicate that the occupation of the $BF_4^-$ sites is not totally random but there is some correlation in the $BF_4^-$ distribution which favors the stoichiometry of $x=0.25$. Although the powder x-ray diffraction does not give any information about this correlation, a possible correlation will be proposed in Sec. IV in order to explain the one dimensionality of the magnetism. When GaPcF is reacted with a larger amount of $NOBF_4$ than the molar ratio of 1:1.5, on the other hand, the x-ray diffraction pattern of the doped phase becomes totally different from that in Fig. 1. The crystal structure in this case is unknown at present.

Futamata *et al.*[9] reported a different crystal structure of GaPcF-$(BF_4)_x$ although their experimental diffraction pattern is almost identical with the present one in Fig. 1. The unit cell they proposed is a tetragonal of $a=3.73$ Å and $b=c=18.94$ Å. With their unit cell, however, it is not possible to index all the reflections. The main reason that led them to the wrong unit cell may be that they did not consider the possibility of the interleaved structure, which gives a correct indexing and a much better fit to the experimental diffraction pattern.

### B. EPR

Figure 3 shows the $K$-band EPR spectrum of the GaPcF-$(BF_4)_{0.25}$ powder, which exhibits a weak $g$ anisotropy characterized by two principal values $g_\parallel$ and $g_\perp$. The EPR signal intensity at 300 K corresponds to the effective spin number of 0.21 per Pc ring. Since there is an antiferromagnetic interaction between the spins, this spin number is consistent with the stoichiometry of GaPcF-$(BF_4)_{0.25}$, and the observed EPR signal is attributed to the localized $GaPcF^+$ radical.

Figure 4 shows the integrated intensity and the peak-to-peak linewidth of the EPR signal as a function of temperature. The EPR signal intensity increases gradually as the temperature is lowered from 300 K and becomes almost constant between 50 and 100 K, and, at $T<20$ K, the signal intensity shows a steep increase. These features suggest that the GaPcF-$(BF_4)_{0.25}$ is a low-dimensional antiferromagnet.[19] A nearly identical result is obtained for the static susceptibility which will be shown in the next subsection. A detailed analysis will be given for the static susceptibility rather than for the EPR signal intensity since the latter has a relatively large experimental error.

The linewidth of the EPR signal shows a gradual temperature dependence without any anomaly. This is also a characteristic of low-dimensional antiferromagnets.[20] As the temperature is lowered, the linewidth increases gradually. This is due to the growth of the short range order which suppresses the exchange narrowing effect. A detailed analysis of the linewidth at $T<15$ K will be given in the next subsection.

### C. Static susceptibility

Figure 5 shows the static susceptibility $\chi$ of the GaPcF-$(BF_4)_{0.25}$ powder. As the temperature is lowered from 300 K, the $\chi$ increases gradually and at 100 K the rate of increase slightly diminishes, and at $T<20$ K the $\chi$ increases steeply. These features are almost identical with those of the EPR signal intensity shown in Fig. 4. The $\chi$ at 290 K is $2.5\times10^{-4}$ emu/mol corresponding to the effective spin number of 0.20 per Pc ring, which also agrees with the EPR result.

In order to elucidate the dimensionality in the magnetism, the $\chi/\chi_c$ vs $T$ plot is shown in Fig. 6, where $\chi_c=Ng^2\mu_B^2S(S+1)/3k_BT$ is the Curie susceptibility. At $T\leqslant15$ K, the $\chi/\chi_c$ is proportional to $T^{0.38}$, i.e., the $\chi$ is proportional to $T^{-0.62}$. At $T\geqslant90$ K, the susceptibility is approximated by the Bonner-Fisher curve[21] with $J=70$ K. Such a temperature dependence of $\chi$, i.e., the $\chi\propto T^{-\alpha}$ $(0\leqslant\alpha\leqslant1)$ dependence at low temperature and the Bonner-Fisher-type dependence at high temperature, is explained by the random-exchange Heisenberg antiferromagnetic chain (REHAC) model of Bondeson and Soos.[22,23]

The REHAC Hamiltonian with an applied field $H$ is

$$\mathcal{H}=\sum_n 2x_nJ\mathbf{S}_n\cdot\mathbf{S}_{n+1}+g\mu_BH\sum_n S_n^z, \tag{1}$$

where $x_nJ$ is the exchange coupling constant between the spins at the sites $n$ and $n+1$, with $x_n$ $(0\leqslant x_n\leqslant1)$ being a random variable representing the disorder. The magnetic behavior of the system is determined by the choice of the dis-

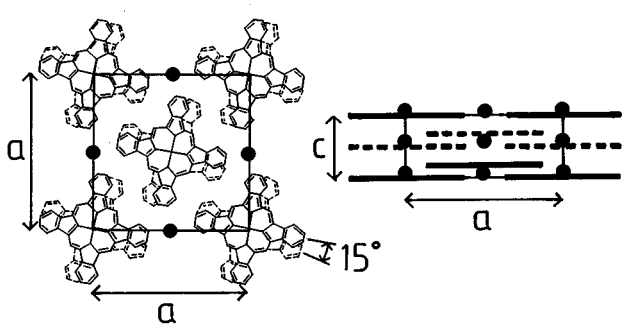


FIG. 2. The crystal structure of GaPcF-$(BF_4)_{0.25}$. The Pc rings shown by the solid and the broken lines are adjacent each other along the $c$ direction. The $BF_4^-$ ions are located randomly at the sites indicated by the filled circles with the probability of 0.25, although the explicit $c$ coordinates of the $BF_4^-$-cites are unknown.

tribution function $f(x)$ for $x_n$. Soos and Bondeson showed that by assuming a distribution function of

$$f(x)=c\,\delta(\epsilon-x)+(1-c)\,\delta(1-x), \tag{2}$$

the susceptibility of quinolinium-$(TCNQ)_2$ and acridinium-$(TCNQ)_2$ is explained for the whole temperature range, where $c$ and $(1-c)$ are the probabilities of weak exchange $\epsilon J$ $(0\leqslant\epsilon<1)$ and strong exchange $J$, respectively. Equation (2) expresses a situation that a uniform chain has occasional weak exchanges resulting in random sequences of even- and odd-length segments that interact weakly with $\epsilon J$. For $k_BT>\epsilon J$, the segments are thermally decoupled each other, and the $\chi$ is characterized by a broad peak centered at $k_BT\sim1.2J$ due to short-range order, which resembles the Bonner-Fisher susceptibility of a regular antiferromagnetic chain. For $k_BT<cJ$, on the other hand, the even- and odd-length segments are frozen into their ground states, i.e., the singlet and the doublet states, respectively. Because of the weak interactions between the odd-length segments, the $\chi$ obeys a $T^{-\alpha}$ $(0\leqslant\alpha\leqslant1)$ law, the exponent $\alpha$ being determined by the $\epsilon$. The crossover between the high- and low-temperature regions occurs at

$$\frac{\chi}{\chi_c}\sim\frac{c}{2-c}. \tag{3}$$

The REHAC model also expects that the EPR linewidth shows a temperature dependence of $\ln(T_0/T)$ in the low-temperature region with $T_0$ being a constant.[24] It is noted that such a behavior of $\chi$ and the EPR linewidth due to the disordered exchange interaction is restricted to the 1D magnet, because, in the two- and three-dimensional magnets, the probability of the appearance of a subsystem weakly interacting with the rest of the system is negligibly small.[25]

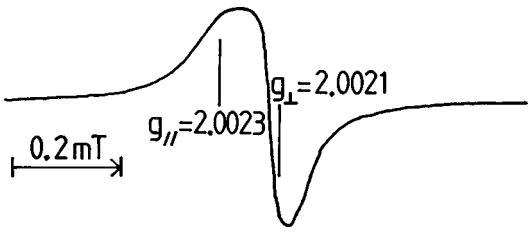


FIG. 3. $K$-band EPR spectrum of GaPcF-$(BF_4)_{0.25}$ powder at 77 K.

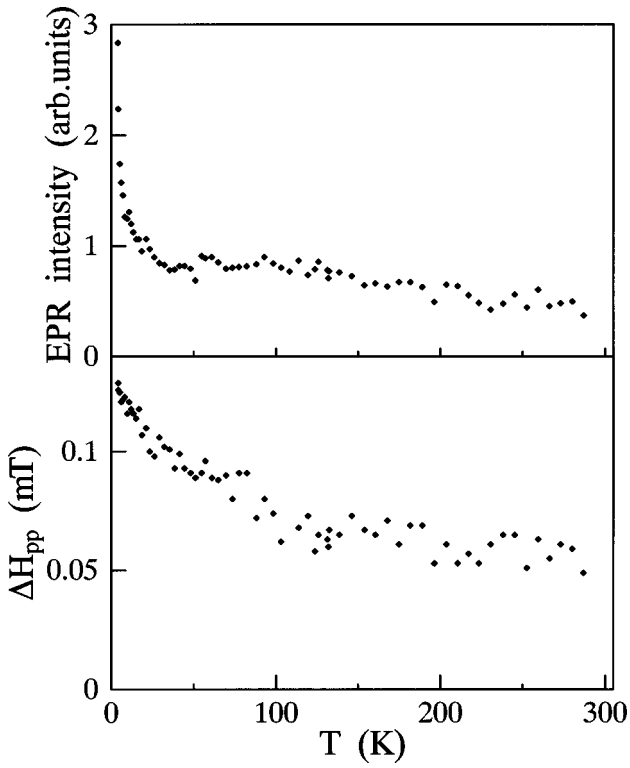


FIG. 4. Temperature dependence of the integrated intensity and the peak-to-peak linewidth of the EPR signal of GaPcF-$(BF_4)_{0.25}$ powder.

The observed temperature dependence of $\chi/\chi_c$ in Fig. 6 is a representation of the REHAC susceptibility. The crossover occurs at $\chi/\chi_c=0.14$, from which it is estimated that $c\sim0.25$. On the other hand, from the observed value of $\alpha=0.62$, it is roughly estimated that $\epsilon\sim$ 0.4 referring to the results of the Bondeson-Soos calculation.[22] Thus, on average, 25 % of the nearest neighbor spins have an interaction of 40% strength compared to the others.

The observed temperature dependence of the EPR linewidth at $T<15$ K is also explained by the REHAC model. Since the present experiment has been done for a powder sample with weak $g$ anisotropy, the observed peak-to-peak linewidth $\Delta H_{pp}$ at the low-temperature region is approximated as

$$\Delta H_{pp}=\Delta H_{aniso}+\Delta H_{REHAC}, \tag{4}$$

where $\Delta H_{aniso}$ is the temperature-independent linewidth due to the $g$ anisotropy, and $\Delta H_{REHAC}$ is the exchange-narrowed dipolar linewidth which is explained by the REHAC model. Following Soos and Bondeson,[24] $\Delta H_{REHAC}$ is the linewidth of an inhomogeneously broadened absorption spectrum:

$$I(\omega)=R^{-1}\sum_{k=1}^{R}I_k(\omega)=R^{-1}\sum_{k=1}^{R}\frac{\chi_k\Gamma_k}{\pi(\omega^2+\Gamma_k^2)}, \tag{5}$$

where $I_k(\omega)$ is the absorption spectrum of the $k$th 1D domain which consists of several segments and $R$ is the number of domains. The essential point is that only the odd-length segments in the domains have nonzero spin 1/2 in their

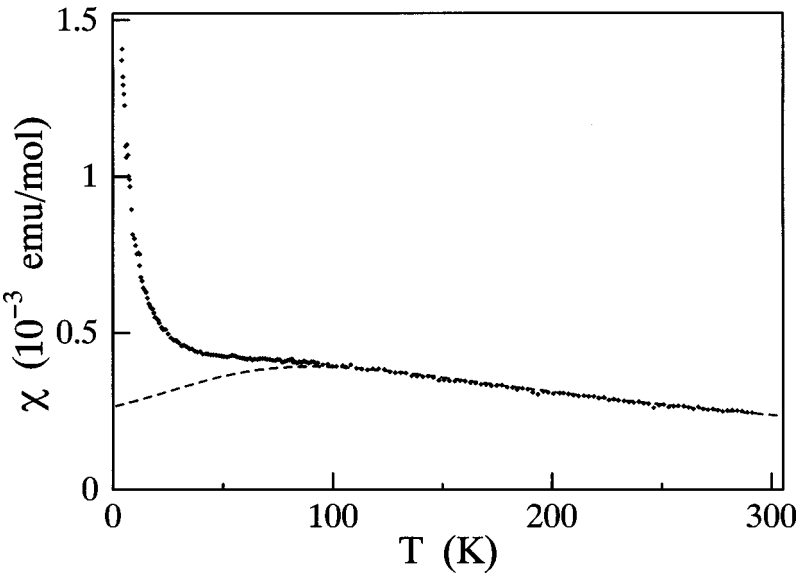


FIG. 5. Static magnetic susceptibility of GaPcF-$(BF_4)_{0.25}$ powder vs temperature. The broken curve is a theoretical one of the Bonner-Fisher susceptibility with $J=70$ K.

ground states at low temperature and that each domain has its characteristic internal exchange field depending on the lengths of the even- and odd-length segments. As a result, the domains have variable linewidth $\Gamma_k$ and susceptibility $\chi_k$. The linewidth $\Gamma_k$ of the $k$th domain at low temperature is written as

$$\Gamma_k(T)=M_2(T)[2\omega_k(T)\omega_\perp(T)]^{-1/2}, \tag{6}$$

with

$$M_2(T)=n(T)M_2(\infty), \tag{7}$$

$$\omega_k(T)=\frac{2J_\parallel}{\hbar}(N-1)^{-1}\sum_{n=1}^{N-1} y_n \exp\left(-\frac{y_nJ_\parallel}{k_BT}\right), \tag{8}$$

$$\omega_\perp(T)=\frac{2J_\perp}{\hbar}[n(T)]^{1/2}. \tag{9}$$

$M_2(T)$ in Eq. (7) is the dipolar second moment with $n(T)=\chi/\chi_c$ in Fig. 6 and $M_2(\infty)$ is the high-temperature second moment. $\omega_k(T)$ in Eq. (8) is the intradomain exchange frequency with $y_nJ_\parallel$ the strength of the exchange interaction between the $n$th and the $(n+1)$th odd-length segments in the $k$th domain and $N$ is the number of the odd-length segments in the domain. The value of $y_n$ is determined by randomly choosing the lengths of the even- and the odd-length segments. $\omega_\perp(T)$ in Eq. (9) represents the interchain exchange frequency with $J_\perp$ the interchain coupling constant at high temperature.

Using the values of $J_\parallel=70$ K, $c=0.25$, and $\epsilon=0.4$, the experimental linewidth at the low-temperature region is fitted with two parameters $\Delta H_{\rm aniso}$ and $M_2(\infty)J_\perp^{-1/2}$. The calculation was done for 3000 domains each of which contains four odd-length segments, i.e., $R=3000$ and $N=4$ in Eqs. (5) and (8). The inset of Fig. 6 shows the experimental and the theoretical linewidth with $\Delta H_{\rm aniso}=0.09$ mT and $M_2(\infty)J_\perp^{-1/2}$

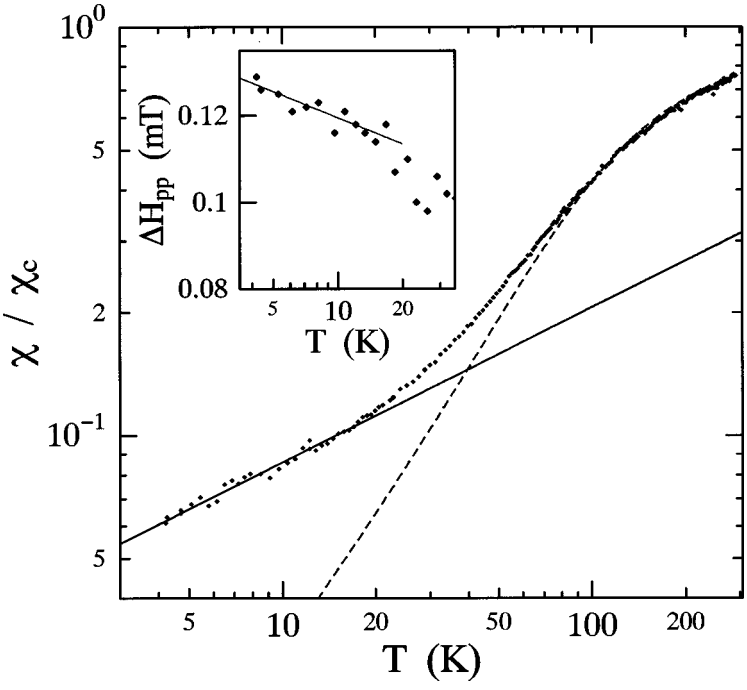


FIG. 6. $\chi/\chi_c$ vs temperature of GaPcF-$(BF_4)_{0.25}$ powder, where $\chi_c$ is the Curie susceptibility. The solid line shows a $\chi/\chi_c \propto T^{0.38}$ line, i.e., $\chi \propto T^{-0.62}$, and the broken curve shows the Bonner-Fisher susceptibility with $J=70$ K. The inset shows the peak-to-peak EPR linewidth vs ln$T$ of the GaPcF-$(BF_4)_{0.25}$ in the low-temperature region. The solid curve in the inset is the theoretical one by the REHAC model, the details of which is described in the text.

$=26\ (\mathrm{mT})^{3/2}$. As is seen in Fig. 6, the experimental temperature dependence of the linewidth at $T<15$ K is well explained by the REHAC model. It is noted that $\Delta H_{\mathrm{REHAC}}$ in Eq. (4) shows a $\log_{10}(T_0/T)$ temperature dependence with $T_0=320$ K in agreement with Soos and Bondeson's result. At $T>15$ K, the abovementioned analysis is no longer applicable since the internal excitation of the spin state occurs in each segment. At this moment, no quantitative analysis is possible for the temperature dependence of the linewidth at $T>15$ K.

In GaPcF-$(BF_4)_{0.25}$, the $BF_4^-$ ions randomly occupy their sites with the probability of 25%, as has been shown in Sec. III A. It is expected that the random occupancy of the $BF_4^-$ sites causes a disorder in the spin alignment along the GaPcF chain, which is the origin of the disordered exchange interaction. In Fig. 6, the crossover is not as sharp as it is in quinolinium-$(TCNQ)_2$ and acridinium-$(TCNQ)_2$,[22] but the crossover region seems to be broadened between 20 and 70 K. This may indicate that the $J$ and the $\epsilon$ in the present system have distributions so that the $\delta$ functions in Eq. (2) should be replaced by other distribution functions of finite widths. The broader distributions may be compatible with the random occupation of the $BF_4^-$ sites. Summarizing, the observed temperature dependence of $\chi$ and the EPR linewidth is explained by the REHAC model, which gives evidence that GaPcF-$(BF_4)_{0.25}$ is a 1D antiferromagnet. The REHAC model is based on a localized spin picture, so that these results give an evidence that the spins are localized in the present system.

The broad peak in the temperature dependence of $\chi$ is expected also in two-dimensional (2D) antiferromagnets.[19] GaPcF-$(BF_4)_{0.25}$ is a 1D antiferromagnet, however, for the following reasons. (a) The $\chi$ and the EPR linewidth at $T<15$ K is explained by the REHAC model which is applicable to the 1D case, but not to the 2D case. (b) If the broad peak in the $\chi-T$ plot corresponds to that of a 2D Heisenberg antiferromagnet, the in-plane exchange coupling constant $J_{2D}$ is estimated to be 47 K using the relation $k_BT(\chi_{\max})/J_{2D}=1.90$ (Ref. 19) with $T(\chi_{\max})=90$ K. The upper limit for the interchain coupling constant, however, is 5 K because of the interleaved structure in the present system, as will be estimated in Sec. IV, so that the $J_{2D}$ value of 47 K is not possible. (c) In most 2D antiferromagnets, the long-range order occurs at $T_N\geqslant 0.5J_{2D}=24$ K.[19] In contrast, no magnetic transition occurs at $T\geqslant 4.2$ K in the present system.

It may seem that the temperature dependence of $\chi$ in Fig. 5 resembles that of AlPcF-I,[3] the latter having a broad peak at $T=80$ K and a sharp increase at $T<20$ K. Definite differences between the two systems are in the EPR results: In the case of AlPcF-I, the EPR intensity disappears and the linewidth diverges at the broad peak of $\chi$. On the other hand, the EPR intensity of GaPcF-$(BF_4)_{0.25}$ shows an almost identical temperature dependence as $\chi$, and the linewidth does not exhibit any anomaly. Furthermore, $\chi$ of AlPcF-I does not show the $\chi\propto T^{-\alpha}$ dependence at the low-temperature region. Thus, the features of the $\chi-T$ curves of the two systems are of totally different origins.

## IV. DISCUSSION

As has been shown in the previous section, GaPcF-$(BF_4)_{0.25}$ (substance A) is a 1D antiferromagnet with $J_\parallel(\mathrm{A})$

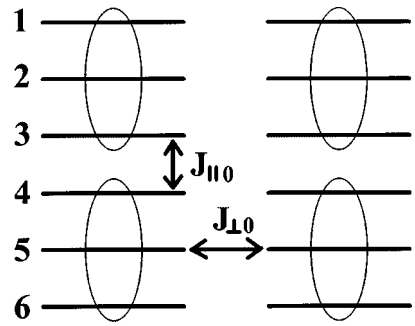


FIG. 7. The spin distribution in AlPcF-I. A spin distributes over three Pc rings, e.g., 1, 2, and 3. $J_{\parallel 0}$ and $J_{\perp 0}$ are the intrachain and the interchain exchange coupling constants when the interacting two spins are localized on the nearest neighbor Pc rings.

$\sim 70$ K and $J_\perp(\mathrm{A})/J_\parallel(\mathrm{A})\ll 1$. On the other hand, AlPcF-I (substance B) shows 3D antiferromagnetism with $J_\parallel(\mathrm{B})\sim J_\perp(\mathrm{B})\sim 30$ K estimated from $T_N$ of 80 K using a mean-field formula.[26] In this section, the relation between the crystal structure and the magnetic dimensionality is discussed.

In AlPcF-I, the density of a spin distributes over three Pc rings along the chain[26] (Fig. 7), which is interpreted as due to the coherence with the charge distribution in the $I_3^-$ array which runs parallel to the Pc chain. Assuming that the spin density distributes evenly for the three Pc rings, e.g. the rings 1, 2 and 3 in Fig. 7, the intrachain and the interchain coupling constants $J_\parallel$ and $J_\perp$ are expressed as follows:

$$J_\parallel(\mathrm{B})=(1/3)^2J_{\parallel 0}(\mathrm{B}), \tag{10}$$

$$J_\perp(\mathrm{B})=J_{\perp 0}(\mathrm{B}), \tag{11}$$

where $J_{\parallel 0}(\mathrm{B})$ and $J_{\perp 0}(\mathrm{B})$ are the coupling constants when the interacting two spins reside on the neighboring two Pc rings along the parallel and perpendicular directions to the chain. The factor $(1/3)^2$ in Eq. (10) is the product of the spin densities at the rings 3 and 4. Since $J_\parallel(\mathrm{B})\sim J_\perp(\mathrm{B})\sim 30$ K, it is estimated that $J_{\parallel 0}(\mathrm{B})\sim 270$ K and $J_{\perp 0}(\mathrm{B})\sim 30$ K.

In the case of GaPcF-$(BF_4)_{0.25}$, the values of $J_{\parallel 0}(\mathrm{A})$ and $J_{\perp 0}(\mathrm{A})$ should be different from those of $J_{\parallel 0}(\mathrm{B})$ and $J_{\perp 0}(\mathrm{B})$. Since AlPcF-I and GaPcF-$(BF_4)_{0.25}$ are considered to be Mott insulators,[6] $J_{\parallel 0}$ is determined using the following formula:[10]

$$J_{\parallel 0}=\frac{2t^2}{U}\rho\left(1-\frac{\sin(2\pi\rho)}{2\pi\rho}\right), \tag{12}$$

where $t$ and $U$ are the transfer integral and the on-site Coulomb energy, respectively, and $\rho$ is the spin density per Pc ring. Whangbo and Stewart showed[27] that $t$ is a function of the inter-ring distance $d$ and the staggering angle $\phi$. Using the values of $d=3.80$ Å and $\phi=15°$ for GaPcF-$(BF_4)_{0.25}$ and $d=3.55$ Å and $\phi=40°$ for AlPcF-I, the ratio $t(\mathrm{A})/t(\mathrm{B})$ is estimated to be 0.60. Since $\rho$ is 0.25 and 0.33 for GaPcF-$(BF_4)_{0.25}$ and AlPcF-I, respectively, and $U$ should be nearly the same for the two substances, it is estimated that $J_{\parallel 0}(\mathrm{A})/J_{\parallel 0}(\mathrm{B})\sim 0.17$, so that $J_{\parallel 0}(\mathrm{A})\sim 46$ K.

$J_{\perp 0}$, on the other hand, is determined by the direct interaction between the neighboring Pc rings through the carbon $\pi$ orbitals in the benzene units of the Pc rings, rather than the superexchange interaction through the intercalated

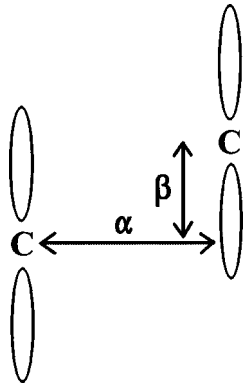


FIG. 8. Definition of the parameters $\alpha$ and $\beta$ in the calculation of the overlap integral between the neighboring carbon $\pi$ orbitals.

anions.[14,28] Since GaPcF-$(BF_4)_{0.25}$ has an interleaved structure, $J_{\perp 0}$ should be substantially diminished. In order to estimate $J_{\perp 0}$ in this case, the overlap integral between the carbon $\pi$ orbitals was calculated for the interleaved and the noninterleaved structures. The parameters used in the calculation are defined in Fig. 8. The distance $\alpha$ is nearly the same for the two substances A and B which is 3.4 Å, while $\beta = 1.57$ Å (interleaved) for A and 0 Å (noninterleaved) for B. The ratio of the calculated overlap integral is $S(\mathrm{A})/S(\mathrm{B}) = 0.18$. Thus, it is roughly estimated that $J_{\perp 0}(\mathrm{A})/J_{\perp 0}(\mathrm{B}) \sim 0.18$, i.e., $J_{\perp 0}(\mathrm{A}) \sim 5$ K. It is noted that $J_{\perp 0}(\mathrm{A}) \sim 5$ K gives the upper limit for the interchain coupling constant in GaPcF-$(BF_4)_{0.25}$ since $J_{\perp 0}$ is for the interaction between the two spins localized on the nearest neighbor Pc rings.

In order to proceed with the estimation of $J_{\parallel}(\mathrm{A})$ and $J_{\perp}(\mathrm{A})$, the knowledge of the spin distribution in the system is indispensable. In the present x-ray diffraction analysis, it was found that the $BF_4^-$ ions occupy their sites randomly with the probability of 0.25. We first consider the case when the $BF_4^-$ distribution is completely random so that the spins distribute randomly in the chains. In this case, the probability that a spin on a Pc ring has the partner spin on the neighboring ring becomes 0.25, so that 25% of the intrachain interactions have a coupling constant of $J_{\parallel}(\mathrm{A}) = J_{\parallel 0}(\mathrm{A}) = 46$ K, and the rest of the interactions have $J_{\parallel}(\mathrm{A}) = 0$, neglecting the second-nearest-neighbor and farther interactions. Similarly, 25% of the interchain interactions have $J_{\perp}(\mathrm{A}) = J_{\perp 0}(\mathrm{A}) = 5$ K and the rest have $J_{\perp}(\mathrm{A}) = 0$. This corresponds to $J = 46$ K, $\epsilon = 0$, and $c = 0.75$ in the REHAC Hamiltonian Eqs. (1) and (2). Although $J = 46$ K is in a correct order compared with the experimental value of $J = 70$ K, $\epsilon$ and $c$ are far different from the experimental values of $\epsilon = 0.4$ and $c = 0.25$. Furthermore, the estimated $J_{\perp}(\mathrm{A})$ value is inconsistent with the experimental estimation of $M_2(\infty) J_{\perp}^{-1/2} \sim 26$ $(\mathrm{mT})^{3/2}$ in Sec. III C: Since the mean interspin distance along the chain becomes $4 \times$(inter-ring distance)$= 15.2$ Å, $M_2(\infty)$ is roughly estimated[26] to be 1 $(\mathrm{mT})^2$, so that $J_{\perp} = 1.5 \times 10^{-3}$ mT$= 1 \times 10^{-6}$ K. This value is totally different from the mean value of the $J_{\perp}(\mathrm{A})$ estimated above, which is $0.25 J_{\perp 0}(\mathrm{A}) \sim 1$ K. Thus the experimental results are not explained by the completely random spin distribution.

As has been mentioned in Sec. III A, the stoichiometry of GaPcF-$(BF_4)_{0.25}$ is stable, which suggests that the distribution of the $BF_4^-$ ions may not be totally random, but there may be some correlation in the distribution. A possible correlation may be such that all the Pc rings have a spin density of 0.25. Figure 9 shows such a $BF_4^-$ distribution. Since the $BF_4^-$ at the site $\gamma$ is surrounded by four Pc rings 1–4, 0.25 spin density is induced evenly on the four Pc rings. Thus, it is assumed that the distribution of the $BF_4^-$ ions in a sheet perpendicular to the $c$ axis is totally periodic but that along the $c$ axis is random. It is noted that this partially correlated $BF_4^-$ distribution explains the experimental x-ray diffraction pattern in Fig. 1 giving almost identical diffraction intensities as those for the completely random $BF_4^-$ distribution. In this case, the intrachain coupling constant $J_{\parallel}(\mathrm{A})$ becomes $J_{\parallel 0}(\mathrm{A})$ since all the spins have their partner spins on the nearest-neighbor Pc rings along the chain. Thus, $J_{\parallel}(\mathrm{A}) = J_{\parallel 0}(\mathrm{A}) = 46$ K. For the interchain interaction, we should consider the interaction between the spins induced by the $BF_4^-$ ions at the sites $\gamma$ and $\delta$. Since the interaction occurs through the Pc rings 3 and 6 or 4 and 5, the coupling constant becomes $J_{\perp}(\mathrm{A}) = 2(1/4)^2 J_{\perp 0} \sim 0.6$ K, where the factor 1/4 is the spin density at a Pc ring and the factor 2 is the number of the interaction paths. Thus, it is expected that $J_{\parallel}(\mathrm{A}) \sim 46$ K and $J_{\perp}(\mathrm{A}) \sim 0.6$ K for the spin distribution in Fig. 9. The value of $J_{\parallel}(\mathrm{A}) \sim 46$ K is in a correct order compared with the experimental value of $J = 70$ K in the REHAC Hamiltonian Eq. (1). The occasional weak exchanges of $\epsilon = 0.4$, estimated in Sec. III C, may be caused by the random distribution of the $BF_4^-$ ions along the $c$ axis which may induce a disorder in the exchange interaction. The estimated value of $J_{\perp}(\mathrm{A}) \sim 0.6$ K is also consistent with the experimental value of $M_2(\infty) J_{\perp}^{-1/2} \sim 26$ $(\mathrm{mT})^{3/2}$: Since the nearest interspin distance is the interring distance 3.8 Å along the chain, $M_2(\infty)$ becomes[26] $\sim 500$ $(\mathrm{mT})^2$, so that $J_{\perp} \sim 370$ mT$\sim 0.25$ K, which is in the same order as the estimated value of $J_{\perp}(\mathrm{A}) \sim 0.6$ K. Thus, the partially correlated $BF_4^-$ distribution in Fig. 9 consistently explains the experimental results.

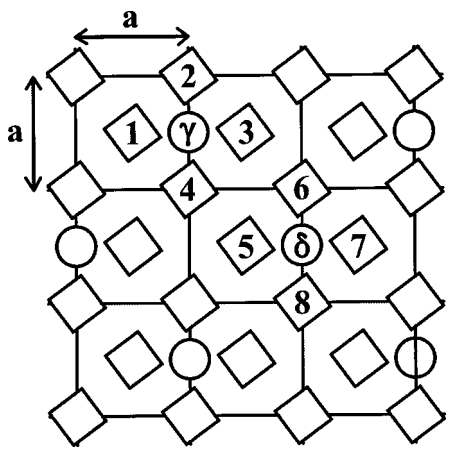


FIG. 9. A partially correlated $BF_4^-$ distribution seen from the $c$ axis. The squares and the circles express the Pc rings and the $BF_4^-$ ions, respectively. The distribution of the $BF_4^-$ is periodic in a sheet perpendicular to the $c$ axis, but that along the $c$ axis is random. This structure induces a spin density of 0.25 on each Pc ring.

With $J_{\perp}/J_{\parallel} \sim 0.01$ and $J_{\parallel} = 70$ K, the long-range order may be expected to occur at $T_N \sim 10$ K using Oguchi's relation,[29] which is not observed in the present system. The

lower $T_N$ in the present system is attributed to the disorder in the exchange interaction with $\epsilon = 0.4$ and $c = 0.25$ estimated in Sec. III C.

## V. CONCLUSIONS

The crystal structure and the magnetism of the GaPcF-$(BF_4)_{0.25}$ powder have been studied. The crystal structure is different from that of AlPcF-I in that the Pc-ring arrays in the neighboring chains have different $c$ coordinates and that the counter anions distribute randomly with a possible partial correlation, which makes GaPcF-$(BF_4)_{0.25}$ a 1D antiferromagnet. The EPR does not show any anomaly between 4.2 and 300 K, indicating that no magnetic transition occurs. The temperature dependence of the static susceptibility $\chi$ as well as the low-temperature EPR linewidth is explained by the REHAC model. These results of the EPR and the $\chi$ measurements indicate that GaPcF-$(BF_4)_{0.25}$ is a 1D antiferromagnet with localized spins.

## ACKNOWLEDGMENTS

This work was supported by a Grant-in-Aid for Scientific Research No. 08640739 from the Japanese Ministry of Education, Science and Culture.

[1] C. J. Schramm, R. P. Scaringe, D. R. Stojakovic, B. M. Hoffman, J. A. Ibers, and T. J. Marks, J. Am. Chem. Soc. **102**, 6702 (1980).
[2] J. Martinsen, S. M. Palmer, J. Tanaka, R. C. Greene, and B. M. Hoffman, Phys. Rev. B **30**, 6269 (1984).
[3] I. Hiromitsu, H. Yamamoto, and T. Ito, Phys. Rev. B **52**, 7252 (1995).
[4] I. Hiromitsu, N. Ikeda, and T. Ito, J. Phys. Soc. Jpn. **66**, 501 (1997).
[5] S. Kitao, M. Seto, Y. Maeda, and I. Hiromitsu, J. Phys. Soc. Jpn. **66**, 850 (1997).
[6] I. Hiromitsu, N. Ikeda, and T. Ito, Synth. Met. **85**, 1737 (1997).
[7] R. S. Nohr and K. J. Wynne, J. Chem. Soc. Chem. Commun. **1981** , 1210.
[8] K. J. Wynne, Inorg. Chem. **24**, 1339 (1985).
[9] M. Futamata and Y. Takaki, Synth. Met. **39**, 343 (1991).
[10] J. B. Torrance, Y. Tomkiewicz, and B. D. Silverman, Phys. Rev. B **15**, 4738 (1977).
[11] J. P. Linsky, T. R. Paul, R. S. Nohr, and M. E. Kenney, Inorg. Chem. **19**, 3131 (1980).
[12] D. C. Weber, P. Brant, R. S. Nohr, S. G. Haupt, and K. J. Wynne, J. Phys. (Paris), Colloq. **44**, C3-639 (1983).
[13] W. A. Rachinger, J. Sci. Instrum. **25**, 254 (1948).
[14] I. Hiromitsu, S. Ohkubo, J. Takeuchi, and T. Ito, Solid State Commun. **89**, 605 (1994).
[15] N. S. Dalal, J. M. Millar, M. S. Jagadeesh, and M. S. Seehra, J. Chem. Phys. **74**, 1916 (1981).
[16] W. Duffy, J. Chem. Phys. **36**, 490 (1962).
[17] N. F. Curtis, J. Chem. Soc. 3147 (1961).
[18] C. W. Dirk, T. Inabe, K. F. Schoch, and T. J. Marks, J. Am. Chem. Soc. **105**, 1539 (1983).
[19] L. J. de Jongh and A. R. Miedema, Adv. Phys. **23**, 1 (1974).
[20] M. Ikebe and M. Date, J. Phys. Soc. Jpn. **30**, 93 (1971).
[21] J. C. Bonner and M. E. Fisher, Phys. Rev. A **135**, 640 (1964).
[22] S. R. Bondeson and Z. G. Soos, Phys. Rev. B **22**, 1793 (1980); Z. G. Soos and S. R. Bondeson, Solid State Commun. **35**, 11 (1980); Z. G. Soos and S. R. Bondeson, in *Extended Linear Chain Compounds*, edited by J. S. Miller (Plenum, New York, 1983), Vol. 3, p. 233.
[23] K. Ikegami, S. Kuroda, M. Saito, K. Saito, M. Sugi, T. Nakamura, M. Matsumoto, and Y. Kawabata, Phys. Rev. B **35**, 3667 (1987).
[24] Z. G. Soos and S. R. Bondeson, Solid State Commun. **39**, 289 (1981).
[25] L. N. Bulaevskii, A. V. Zvarykina, Yu. S. Karimov, R. B. Lyubovskii, and I. F. Shchegolov, Sov. Phys. JETP **35**, 384 (1972).
[26] I. Hiromitsu, N. Ikeda, H. Yamamoto, and T. Ito J. Phys. Soc. Jpn. **64**, 4935 (1995).
[27] M.-H. Whangbo and K. R. Stewart, Isr. J. Chem. **23**, 133 (1983).
[28] I. Hiromitsu, S. Ohkubo, J. Takeuchi, and T. Ito, J. Phys. Soc. Jpn. **63**, 2716 (1994).
[29] T. Oguchi, Phys. Rev. A **133**, 1098 (1964).